criminating ability of the intermediate, $[Fe(CO)_3C(OC_2H_5)CH_3]$, for triphenylphosphine *vs.* other phosphorus ligands (L′). These data also indicate that the four-coordinate species $[Fe(CO)_3C(OC_2H_5)CH_3]$ has a greater propensity for more nucleophilic ligands, the order of preference being: $(n\text{-}C_4H_9)_3P$ (2.9) > $(C_6H_{11})_3P$ (1) ≈ $(C_6H_5)_3P$ (1) > $P(OC_6H_5)_3$ (0.31). This is the usual observed order of nucleophilicity for these ligands.[2a] The fact that $(C_6H_{11})_3P$ is not more reactive toward the four-coordinate intermediate is presumably a result of the bulkiness of the cyclohexyl rings.

Therefore, the intermediate $[Fe(CO)_3C(OC_2H_5)CH_3]$ shows a significant preference (about 10:1) for the more nucleophilic ligand $(n\text{-}C_4H_9)_3P$ as compared with the more electrophilic ligand $(C_6H_5O)_3P$.[35] This is in contrast to the nature of the $[Mo(CO)_4P(C_6H_5)_3]$ intermediate produced from the corresponding amine complex which, although it is fairly nondiscriminating, shows a greater preference for electrophilic ligands: $P(OCH_2)_3CC_2H_5$ (1.62) > $P(C_6H_5)_3$ (1) > $P(n\text{-}C_4H_9)_3$ (0.68).[5]

Acknowledgment. The authors are particularly grateful for the help of their colleague, Dr. M. York Darensbourg, who initiated this project. In addition, we wish to express our thanks to the donors of the Petroleum Research Fund, administered by the American Chemical Society, for financial support of this project and to Research Corporation for a Cottrell Research Grant awarded to M. Y. Darensbourg and D. J. Darensbourg for the purchase of a Perkin-Elmer 521 infrared spectrophotometer.

Registry No. $P(C_6H_5)_3Fe(CO)_3C(OC_2H_5)C_6H_5$, 42947-52-4; $P(OC_6H_5)_3Fe(CO)_3C(OC_2H_5)C_6H_5$, 42947-53-5; $P(C_6H_5)_3Fe(CO)_3C(OC_2H_5)CH_3$, 42947-54-6; $P(OC_6H_5)_3Fe(CO)_3C(OC_2H_5)CH_3$, 42947-55-7; $P(C_6H_{11})_3Fe(CO)_3C(OC_2H_5)CH_3$, 42947-56-8; $P(n\text{-}C_4H_9)_3Fe(CO)_3C(OC_2H_5)CH_3$, 42947-57-9; $P(OC_6H_5)_3$, 101-02-0; $P(n\text{-}C_4H_9)_3$, 998-40-3; $P(C_6H_5)_3$, 603-35-0; $P(C_6H_{11})_3$, 2622-14-2.

[35] G. Cardaci and V. Narciso, *J. Chem. Soc., Dalton Trans.*, 2289 (1972), have found the intermediate $[Fe(CO)_4]$ species produced *via* dissociation of $CH_2{=}CHX$ from $(CH_2{=}CHX)Fe(CO)_4$ ($X = OC_2H_5$, C_4H_9, C_6H_5, CO_2CH_3, and CN) complexes to be fairly nondiscriminating toward $CH_2{=}CHX$ ligands *vs.* carbon monoxide.

Contribution from the Department of Chemistry,
Case Western Reserve University, Cleveland, Ohio 44106

Kinetics of Iron(III) Interactions with Phenol and *o*-Aminophenol

SHARON GOUGER and JOHN STUEHR*

Received April 16, 1973

Kinetic measurements by the stopped-flow technique are reported at 25° and $I = 0.1$ for the reaction of Fe(III) with phenol and *o*-aminophenol. For phenol, close-to-equilibrium data indicate a reaction mechanism involving the reaction of the protonated ligand with both Fe^{3+} and $FeOH^{2+}$ (second-order rate constants measured to be 25 and 720 M^{-1} sec^{-1}). The data for *o*-aminophenol on the other hand are consistent with the reaction of $FeOH^{2+}$ with the monoprotonated ligand ($k = 1.1 \times 10^5$ M^{-1} sec^{-1}). The present results are compared with previous measurements involving a wide variety of ligands in an attempt to resolve questions of "proton ambiguity."

Introduction

Of all the first-row transition metal ions, Fe(III) has been one of the most difficult to study kinetically. This has been due to the fact that the free metal ion readily hydrolyzes,[1,2] even in moderately acid solutions, to $FeOH^{2+}$, which can dimerize.[3] In addition, the complexing ligand can react with either the free ion or the $FeOH^{2+}$ species, or both.[4] If the ligand itself can exist in free and protonated forms, the number of mechanistic pathways quickly proliferates. Complexation pathways, involving the protonated and unprotonated ligands, have been found for both Fe^{3+} and $FeOH^{2+}$. Of the kinetic studies that have been carried out with Fe(III), the majority have involved "simple" ligands[4-6] such as Cl^- and Br^- which only attack in the anionic form or ligands[7,8] such as SCN^- and SO_4^{2-} which can react either in the singly protonated or in unprotonated forms. Only recently have bidentate or biprotonated ligands such as salicylic acid and analogs[9] been utilized. In many of these studies, the data could be interpreted on the basis of two or more kinetically ambiguous mechanisms, *e.g.*, by pathways involving Fe^{3+} + L or $FeOH^{2+}$ + HL. In such instances, it was necessary to choose between possible alternatives by examining the "reasonableness"[10] of the rate constants obtained. The purpose of this work was to carry out similar studies with ligands of sufficiently high p*K* values such that kinetic contributions from the free ligand were negligible. For this purpose we chose phenol ($pK_a = 9.8$) and *o*-aminophenol ($pK_1 = 4.9$, $pK_2 \approx 9.8$).

Experimental Section

Materials. *o*-Aminophenol was added to saturation to about 100 ml of hot 95% ethanol under a nitrogen atmosphere. Activated charcoal was stirred in until the solution became colorless, after which the clear hot solution was quickly filtered and then refrigerated until all the crystals had formed. The white crystals were filtered, washed with hexane, and stored under nitrogen until used. Fisher reagent grade $Fe(NO_3)_3 \cdot 9H_2O$ and KNO_3 were used without further purification. Phenol was purified by distillation.

[1] R. Arnek and K. Schylter, *Acta Chem. Scand.*, 22, 1327 (1968).

[2] M. Eigen and R. G. Wilkins, *Advan. Chem. Ser.*, No. 49, 55 (1965); see also M. Eigen, *Pure Appl. Chem.*, 6, 97 (1963).

[3] (a) H. Wendt, *Inorg. Chem.*, 8, 1527 (1969); (b) B. A. Sommar and D. W. Margerum, *ibid.*, 9, 2517 (1970).

[4] R. E. Connick and C. P. Coppel, *J. Amer. Chem. Soc.*, 81, 6389 (1959).

[5] P. Matthies and H. Wendt, *Z. Phys. Chem. (Frankfurt am Main)*, 30, 137 (1961).

[6] T. Yasunaga and S. Harada, *Bull. Chem. Soc. Jap.*, 42, 2165 (1969).

[7] J. F. Below, R. E. Connick, and C. P. Coppel, *J. Amer. Chem. Soc.*, 80, 2961 (1958).

[8] F. P. Cavasino, *J. Phys. Chem.*, 72, 1378 (1968).

[9] (a) G. Saini and E. Mentasti, *Inorg. Chim. Acta*, 4, 585 (1970); (b) *ibid.*, 4, 210 (1970).

[10] J. H. Espensen and D. F. Dustin, *Inorg. Chem.*, 8, 1760 (1969).

All solutions were prepared fresh daily and maintained at $I = 0.1$ with 0.1 M KNO_3. Acid concentrations were adjusted to between 0.005 and 0.05 M with HNO_3. For *o*-aminophenol, all solutions were degassed and then saturated with high-purity nitrogen. Solutions of *o*-aminophenol typically discolored in less than 0.5 hr in contact with air, so all stopped-flow measurements were made within this period.

Instrumentation. The pH's of the initial solutions were adjusted by dropwise additions of KOH and/or HNO_3 and measured on a Beckman Expandomatic pH meter. Kinetic runs were made on the Gibson-Durrum stopped-flow spectrophotometer. Transmittance of light as a function of time was monitored on an oscilloscope as the components reacted. Traces were photographed from the oscilloscope by a Polaroid camera.

Treatment of Data. For the phenol experiments, relaxation times were computed using close-to-equilibrium data. Equilibrium concentrations for all species present were obtained from a standard computer program. Since the stability constants for complexation of trivalent iron and *o*-aminophenol are not known, close-to-equilibrium or relaxation kinetics could not be used as a method of analysis. The kinetic curves were converted to absorbance and plotted against time, from which the initial rate of absorbance change was obtained. Holding all else constant, but varying the concentration of *o*-aminophenol, and plotting the logarithm of the rates against the logarithm of the corresponding concentrations gave the order of the reaction with respect to *o*-aminophenol. This was also done for the iron and proton dependences. Logarithms of equilibrium constants may be found in Table I.

The range of initial concentrations utilized in these studies was from 0.0005 to 0.008 M in *o*-aminophenol, from 0.005 to 0.04 M in phenol, and from 0.0005 to 0.0125 M in $Fe(NO_3)_3$. The pH of the solutions was varied from 1.4 to 2.4. Half-times for the phenol runs were from about 1.5 to 2.6 msec. For *o*-aminophenol, half-times were much longer, typically 10–50 sec.

Results

Phenol. The kinetic data were obtained on the stopped-flow spectrophotometer at 550 nm. Concentration data and relaxation times are given in Table II. The phenol effect could be studied over only a relatively narrow range of experimental conditions. As the concentration of H^+ was increased, the half-times became shorter, approaching the ultimate resolution of the instrument.[11] At lower concentrations, the amplitudes of the effect decreased. Even so, it is clear that at fixed iron and phenol concentrations, the process became *slower* as the pH was increased. No significant variation of τ with overall iron or phenol concentrations could be detected.

The mechanism consistent with the data is the dual-pathway mechanism A in which both Fe^{3+} and $FeOH^{2+}$ react with the protonated phenol

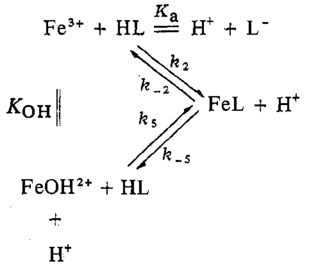

(A)

where the proton-transfer steps (represented by equal signs) are considered rapid. This is similar to that found by several other workers[8,12,13] for trivalent iron complexation reactions. Kinetic pathways involving reaction with the free ligand (L^-) were not consistent with the observed relaxation times. The concentrations of the anionic form of phenol were so small (~10^{-8} times the total ligand concentration) that the rate constants would have to be on the order of 10^{12} M^{-1} sec^{-1}, which is much larger than the diffusion-controlled limit. The relaxation time for (A) is given by

$$\frac{1}{\tau} = k_2\left[[Fe^{3+}]\frac{\alpha - y([L]/K_a)}{1+\alpha} + [HL]y\right] + k_{-2}\left[[FeL^+]\frac{y([H^+]/K_a) + (y-1)}{1+\alpha} + [H^+]\right] + k_5\left[[FeOH^{2+}]\left[z(1+\beta) - \frac{K_{OH}}{[FeOH]}\right] + [HL]z\right] + k_{-5} \quad (1)$$

where

$$y = \frac{\dfrac{[FeOH^{2+}]}{1+\alpha} + [H^+]}{\left(1 + \dfrac{[H^+]}{K_a}\right)\dfrac{[FeOH^{2+}]}{1+\alpha} + K_{OH} + [H^+]}$$

$$z = \frac{\dfrac{[H^+]}{K_a}\dfrac{[FeOH^{2+}]}{1+\alpha} + K_{OH}}{\left(1 + \dfrac{[H^+]}{K_a}\right)\dfrac{[FeOH^{2+}]}{1+\alpha} + K_{OH} + [H^+]}$$

$$\alpha = ([H^+] + [L])/K_a$$

$$\beta = (K_{OH} + [H^+])/[FeOH^{2+}]$$

and the chemical symbols in brackets represent equilibrium

Table I. Logarithms of Equilibrium Constants[a] ($I = 0.1$, 25°)

	log K	
Reaction	Phenol	*o*-Aminophenol
$H_2L^+ \rightleftharpoons H^+ + LH$		−4.86 (K_{a1})
$HL \rightleftharpoons H^+ + L^-$	−9.78	−9.79 (K_{a2})[b]
$Fe^{3+} + L^- \rightleftharpoons FeL^{2+}$	7.57[b]	
$Fe^{3+} + H_2O \rightleftharpoons FeOH^{2+} + H^+$	−2.63 (K_{OH})	

[a] All data taken from L. Sillen and A. Martell, *Chem. Soc., Spec. Publ.*, No. 17 (1964), or No. 25 (1971). [b] Values at $I = 0$ were adjusted to $I = 0.1$ by means of the extended Debye-Huckel equation.

Table II. Kinetic Data for the Fe(III)-Phenol System at 25° and $I = 0.1$

$[Fe^{3+}]_\Sigma$,[a] M	$[L]_\Sigma$,[a] M	pH[b]	τ, msec
0.00625	0.005	1.40	2.2
0.00625	0.01	1.40	2.2
0.00625	0.02	1.40	2.2
0.00625	0.04	1.40	2.3
0.00625	0.02	1.67	2.5
0.0125	0.02	1.95	2.7
0.00625	0.02	1.99	2.8
0.00313	0.02	2.00	3.2
0.00625	0.02	2.00	3.3
0.0125	0.02	2.00	3.1
0.00063	0.02	2.01	3.0
0.00625	0.005	2.01	3.0
0.00625	0.02	2.02	2.8
0.0125	0.04	2.18	3.7
0.000625	0.02	2.18	3.3
0.00625	0.02	2.18	3.4
0.00625	0.04	2.20	3.7
0.00625	0.02	2.21	3.2
0.00625	0.005	2.22	3.5

[a] Overall concentrations. [b] Equilibrium pH values were converted to C_H from a_H by $\gamma_H = 0.82$.

---

(11) The time resolution with 2-cm optical path length is estimated to be 0.8 msec, even though the "dead time" (elapsed time between mixing and observation) is about 2 msec. In order to resolve times less the latter, the optical changes must be quite large.

(12) D. Seewald and N. Sutin, *Inorg. Chem.*, 2, 643 (1963).

(13) F. Accascina, F. P. Cavasino, and S. D'Alessandro, *J. Phys. Chem.*, 71, 2474 (1967).

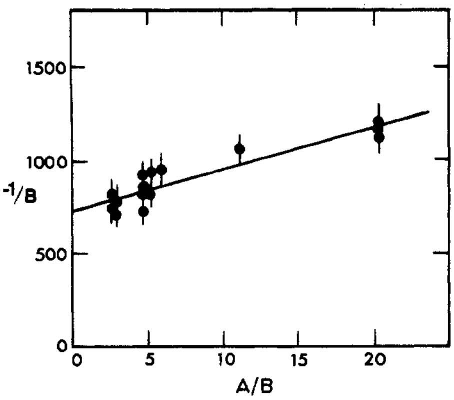

Figure 1. Concentration and pH dependence of the relaxation time for the reaction of Fe(III) with phenol.

concentrations. The y and z factors result from the rapid proton-transfer preequilibria involving K_a and K_{OH} in (A). Although eq 1 is rather complicated as written, in practice it simplifies considerably. Numerically, $y \cong 1, \beta >> 1, \alpha >>> 1$, $[L]/K_a \cong 1$ such that eq 1 reduces to

$$\frac{1}{\tau} = k_2\{[Fe^{3+}] + [HL] + (1/K_2)([FeL^{2+}] + [H^+])\} + k_5\{[FeOH^{2+}](1+\beta)z + [HL]z + 1/K_5\} \quad (2)$$

$$\frac{1}{\tau} = k_2A + k_5B$$

where A and B are the terms in the braces in eq 2. It is evident from these terms why the relaxation time was relatively insensitive to metal and ligand concentrations but decreased with increasing hydrogen ion concentration. The quantity $1/K_5$ constitutes the majority of B; the latter thus varies only slightly with concentration. In the factor identified as A, $1/K_2 = 156$; as a consequence, the concentration dependence of A is given by $[FeL^{2+}] + [H^+] \cong [H^+]$. A graph of τ^{-1}/B *vs.* A/B yields a straight line (Figure 1), from which the values of k_2 and k_5 are obtained as the slope and intercept, respectively. The results are $k_2 \cong 25\ M^{-1}$ sec^{-1} and $720\ M^{-1}$ sec^{-1} (Table IV). The value of k_2 is only approximate, since τ^{-1}/A varied by less than a factor of 2 over the entire pH range studied and each point in Figure 1 may be regarded as uncertain by 10-15%. The slope in fact could be considerably less than that given by the line in Figure 1.

***o*-Aminophenol.** For the Fe^{3+}-*o*-aminophenol system, a single kinetic process much slower than that for phenol was observed. The optical density changes were quite large over the entire wavelength range available; 600 nm proved to be a convenient observation wavelength.

The kinetic effect was found by the method of initial rates to be first order in total *o*-aminophenol and first order in total iron at a fixed pH. That is, the empirical rate law has the form, at constant $[H^+]$

$$\text{rate} = k_{app}[Fe^{III}]_\Sigma[H_2L]_\Sigma \quad (3)$$

This is a simple second-order equation which may be integrated, in terms of the measured absorbance values, to

$$\ln\frac{(b/a)(A_\infty - A)}{(A_\infty - A_0)(b/a) - (A - A_0)} = k_{app}(a-b)t \quad (4)$$

where A_0 and A_∞ are the $t = 0$ and $t = \infty$ absorbance values and b and a are the reactant initial concentrations (defined such that $b > a$). At fixed pH values, the left-hand side of eq 4 was graphed *vs.* time, yielding $k_{app}(a-b)$ as the slope.

Table III. Values of k_{app} for the Fe(III)-*o*-Aminophenol Reaction[a]

$[Fe^{3+}]_\Sigma$,[b] M	$[L]_\Sigma$,[b] M	pH	k_{app}, M^{-1} sec^{-1}
0.00125	0.0005	2.00	21
0.00125	0.001	2.00	52[c]
0.00125	0.002	2.05	34
0.00125	0.008	2.01	25
0.00025	0.001	2.07	40
0.0005	0.001	2.04	51[c]
0.0025	0.001	2.00	25
0.005	0.001	1.92	20
0.00125	0.004	1.61	5
0.00125	0.004	1.67	12
0.00125	0.004	1.97	32
0.00125	0.004	2.17	70
0.00125	0.004	2.39	121
0.00125	0.004	2.45	169

[a] At 25° and $I = 0.1\ M$. [b] Stoichiometric concentrations. [c] Values of k_{app} computed by dividing the slope of eq 4 by $(a-b)$ are subject to larger errors when a and b are not very different.

The slopes were then graphed *vs.* $a - b$, which yielded straight lines at each pH. At pH 2.00, the value of k_{app} was 25.5 M^{-1} sec^{-1}. The stability constant for the Fe(III)-*o*-aminophenol system, although not known, appears to be sufficiently large such that no contributions from the reverse reaction could be detected.

See Table III for values of k_{app} for the Fe(III)-*o*-aminophenol reaction.

We turn our attention now to the hydrogen ion dependence of the rate. There are in principle six reaction paths involving the species Fe^{3+}, $FeOH^{2+}$, H_2L^+, HL, and L^- [14]

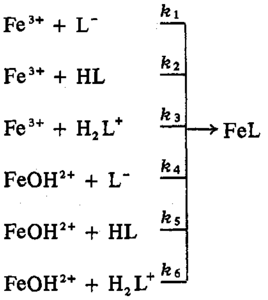

(B)

The total rate law from this reaction scheme is given by

$$d[FeL]/dt = k_{app}[Fe^{III}]_\Sigma[H_2L]_\Sigma \quad (5)$$

where

$$k_{app} = \frac{k_1K_1K_2}{1 + K_{OH}/[H]}\left(\frac{1}{[H]^2}\right) + \frac{k_2K_1}{1 + K_{OH}/[H]}\left(\frac{1}{[H]}\right) + \frac{k_3}{1 + K_{OH}/[H]} + \frac{k_4K_{OH}K_1K_2}{1 + K_{OH}/[H]}\left(\frac{1}{[H]^3}\right) + \frac{k_5K_{OH}K_1}{1 + K_{OH}/[H]}\left(\frac{1}{[H]^2}\right) + \frac{k_6K_{OH}}{1 + K_{OH}/[H]}\left(\frac{1}{[H]}\right) \quad (6)$$

and K_{OH}, K_1, and K_2 are the dissociation constants defined in Table I. That is, the various reaction pathways predict several different hydrogen ion dependences ranging from zero to inverse third power. The quantity $K_{OH}/[H]$ accounts for the hydrolysis equilibrium involving the metal ion. We were able to test our data for its dependence on hydrogen ion con-

---

(14) The free protons interrelating the various species are not shown for simplicity.

Table IV. Summary of Rate Constants (M^{-1} sec^{-1}) for Various Fe(II) Pathways

		Reaction				
Ligand[a]	I	$Fe^{3+} + L$ k_1	$Fe^{3+} + HL$ k_2	$FeOH^{2+} + L$ k_4	$FeOH^{2+} + HL$ k_5	Ref
Cl^-	1.0	9.4		1.1×10^4		*d*
	1.0	19		1.2×10^4		*e*
Br^-	1.0	50		4.1×10^4		*e*
	1.7	20		2.6×10^4		*f*
$Fe(CN)_6^{3-}$	0.5	1750				*g*
SCN^-	0.4	127		1.0×10^4		*h*
$H_2PO_2^-$	1.0	270	13		2.1×10^4	*i*
SO_4^{2-}	0.5	(6.4×10^3)			1.4×10^5	*j*
		1×10^3		3×10^5	3×10^4	*k*
	0.5	$(3.5\text{-}4.6) \times 10^3$	38	1.1×10^5	5×10^4	*l*
F^-	0.5	(4×10^3)	11		3.1×10^3	*m*
CH_2ClCO^-	1.0	(4.9×10^3)	2.2	2.8×10^4	6.8×10^3	*n*
N_3^-	1.0	(1.6×10^5)	4.0		6.8×10^3	*o*
	0.1			$\sim 3 \times 10^3\text{-}\sim 4 \times 10^4$	7.4×10^3	*p*
	1.0	(1.4×10^5)	2.6		6.1×10^3	*q*
CH_3COO^-	1.0	(3.4×10^5)	4.8		5.3×10^3	*n*
$CH_3CH_2COO^-$	1.0	(4.2×10^5)	5.7		5.1×10^3	*n*
CrO_4^{2-}	1.0	(5×10^7)			9.2×10^3	*r*
$C_6H_5O^-$	0.1	*b*	~ 25		7.2×10^2	*s*
$C_6H_4(NH_2)O^-$	0.1	*b*			1.1×10^5	*s*
$SSal^{3-}$	1.0	*b*	1.8×10^3		1.2×10^4 [c]	*t*
Sal^{2-}	1.0	*b*			1.4×10^4 [c]	*u*

[a] L form shown. [b] Values, if computed, would exceed the diffusion-controlled limit. [c] Reaction pathways involving H_2L were also reported. [d] Reference 4. [e] Reference 6. [f] Reference 5. [g] D. L. Singleton and J. H. Swinehart, *Inorg. Chem.*, 6, 1536 (1967). [h] Reference 7. [i] Reference 10. [j] G. G. Davis and W. M. Smith, *Can. J. Chem.*, 40, 1836 (1962). [k] H. Wendt and H. Strehlow, *Z. Elektrochem.*, 66, 228 (1962). [l] Reference 8. [m] D. Pouli and W. M. Smith, *Can. J. Chem.*, 38, 567 (1970). [n] F. Accascina, F. P. Cavasino, and E. DiDio, *Trans. Faraday Soc.*, 65, 489 (1969). [o] Reference 12. [p] Reference 13. [q] D. W. Carlyle and J. H. Espenson, *Inorg. Chem.*, 6, 1370 (1967). [r] J. H. Espenson and S. R. Helzer, *ibid.*, 8, 1051 (1969). [s] This work. [t] Reference 9b. [u] Reference 9a.

centration and found that only the terms involving $1/[H]^2$ were significant. A simultaneous test for the $1/[H]$ and $1/[H]^2$ terms, for example, is obtained by graphing $k_{app}(1 + K_{OH}/[H])[H]$ *vs.* $1/[H]$, Figure 2. The intercept of this graph is $k_2K_1 + k_6K_{OH}$ and the slope is $k_1K_1K_2 + k_5K_{OH}K_1$. Experimentally, we find the intercept to be 0.04 ± 0.04. That is, within experimental error the graph passes through the origin, indicating that contributions from paths 2 and 6 are small. Actually, if one identifies the maximum possible intercept with k_2K_1 (the more likely contributor), the resulting k_1 value ($\leqslant 5 \times 10^3$ M^{-1} sec^{-1}) is unrealistically large for a 3-1 charge type (see Table IV). Similar graphs eliminated significant contributions from paths 3 and 4. We are then left with the conclusion that the slope of Figure 2 is

$$k_1K_1K_2 + k_5K_{OH}K_1 = 4.4 \times 10^{-3}\ M^{-1}\ \text{sec}^{-1} \qquad (7)$$

Steps 1 and 5 have the same predicted hydrogen ion dependence; they suffer from formal "proton ambiguity" in that one cannot distinguish between the two paths by means of pH alone. On the other hand, if one solves for k_1 from eq 7 with the values of K_1 and K_2 from Table I, there results $k_1 = 2 \times 10^{12}$ M^{-1} sec^{-1}, some two orders of magnitude larger than the diffusion-controlled limit for a bimolecular reaction. It is thus apparent that since pathway 1 can make only a negligible contribution, the rate is determined essentially by path 5 alone. With this conclusion one can unambiguously compute k_5 to be 1.1×10^5 M^{-1} sec^{-1}.

Discussion

The mechanism for complex formation may be separated into two parts according to the Eigen-Tamm mechanism[15]

$$Fe^{z+} + L \overset{K_{os}}{=\!=} FeOH_2 \cdot L \xrightleftharpoons{k_{1p}} FeL + H_2O \qquad (C)$$

where Fe^{z+} indicates either $Fe(OH_2)_6^{3+}$ or $Fe(OH_2)_5OH^{2+}$.

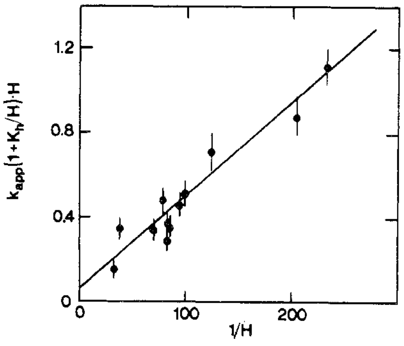

Figure 2. Test of the $1/[H]$ and $1/[H]^2$ pathways *via* eq 6 for the reaction of Fe(III) with *o*-aminophenol. The error bars include uncertainties in k_{app} as well as in $[H^+]$.

The first step involves the very rapid formation of an outer-sphere complex, in which the metal and ligand are separated by one or more water molecules. The equilibrium constant for this step is designated as K_{os} and is a function of the charge type of the electrostatic interaction. This step is followed by the rate-determining formation of the inner-sphere complex, characterized by the ligand penetration rate constant k_{1p}. The relation between the latter and the overall measured rate constant k_{obsd} is $k_{obsd} = K_{os}k_{1p}$.

A number of workers[6,8,12,13,16] have attempted to correlate data from different laboratories and to come to some conclusion as to the mechanism of substitution on Fe(III). The principal difficulty is that many of the systems involving ligands with dissociable protons are characterized by "proton ambiguity" as described earlier; *i.e.*, the reaction path $FeOH^{2+} + HL$ cannot be kinetically distinguished from $Fe^{3+} + L^-$. Analysis of the data *via* either pathway often gave physically possible rate constants. The only way of distinguishing be-

---

(15) M. Eigen and K. Tamm, *Z. Elektrochem.*, 66, 93, 107 (1962).

(16) P. G. T. Fogg and R. J. Hall, *J. Chem. Soc. A*, 1365 (1971).

tween the two was to make some judgement about the "reasonableness" of the rate constants.

Table IV summarizes much of the kinetic data available as of 1973 in Fe(III) systems. The discussion which follows is concerned with the ambiguity between the k_1 and k_5 values. The former are written in parentheses to emphasize the fact that both sets of numbers cannot be simultaneously correct. Several features of this table warrant particular attention. First, when several laboratories report data on the same system and observe the same hydrogen ion dependence in the rate law, the agreement as to numerical rate constants is generally satisfactory when differences in conditions are taken into account. Second, it is possible for different investigators to come to different conclusions as to which pathways are present (quite aside from the proton ambiguity question). For example, kinetic data from various laboratories[17,18] have been interpreted as being consistent with the k_1 pathway for SO_4^{2-}, but a detailed study by Cavasino[8] indicated that simultaneous contributions were being made by pathways 1, 2, and 4. A similar disagreement exists with azide. Unless there is agreement as to which hydrogen ion dependences are present in the rate laws, it is of course not possible even to address the question of resolving the proton ambiguity. Third, some of the systems in Table V involve ligands which do not protonate under ordinary conditions (Cl^-, Br^-, SCN^-). For these, the rate constants may be unambiguously assigned to one or more pathways in reaction B.

Several groups of investigators have examined rate data for Fe(III) systems and attempted to resolve the proton ambiguity on logical grounds. Seewald and Sutin[12] were among the first to point out that if the ambiguous rates were assigned to pathway 1 of reaction scheme B, then rate constants varied considerably from ligand to ligand. If, on the other hand, the data were assigned to pathway 5, then the ligand dependence was very much reduced. They preferred the latter assignment, noting however that either was completely consistent with the data.

More recently, Fogg and Hall[16] computed the values of k_{1p} (from $k_{1p} = k/K_{os}$) and correlated them with ligand basicity. If the ambiguous reactions studied as of that time were interpreted on the basis of pathway 1, they noted that the values of k_{1p}, for charged or uncharged ligand, increased with increasing basicity of the ligand. The range was from $k_{1p} = 9.0$ sec^{-1} for Cl^- ($pK_a \cong -7$) to 9.5×10^5 sec^{-1} for salicylaldehyde ($pK_a \cong 9.5$). Fogg and Hall interpreted this as suggesting an associative mechanism in which the ligand abstracts a proton from a water molecule in the primary hydration sphere of $Fe(H_2O)_6^{3+}$, followed by substitution of the protonated ligand into the inner sphere of the metal ion.

On the other hand, if they interpreted the rate data on the basis of the other possibility (pathway 5 in reaction scheme B), some ligand dependence was still noted, but it was considerably less. The variation of k_{1p} was between 3×10^3 and 3×10^4 sec^{-1}. In fact, the ligands appeared to have "little influence" on the values of k_{1p} for the FeOH pathway. Fogg and Hall suggested this was an SN1 dissociative mechanism, the rate-determining step being the release of a water molecule followed by a rapid coordination reaction. No definite conclusion was reached as to which of these explanations was the correct one.

Table V. Ligand Penetration Rate Constants[a] for Pathways 1 and 5

		Reaction	
Ligand[b]	pK_a	$Fe^{3+} + L$ k_{1p}, sec^{-1}	$FeOH^{2+} + HL$ $10^{-4}k_{1p}$, sec^{-1}
Cl^-		4	
Br^-		4	
$Fe(CN_6)^{3-}$		50[c]	
SCN^-	−1.8	30	
$PO_2H_2^-$	1.1	(50)	7
SO_4^{2-}	1.4	(400)	2
F^-	2.9	(800)	1
CH_2ClCOO^-	2.9	(1×10^3)	2
N_3^-	4.6	(3×10^4)	2
CH_3COO^-	4.8	(7×10^4)	2
$C_2H_5COO^-$	4.8	(8×10^4)	2
CrO_4^{2-}	6.6	(5×10^5)	0.3
$C_6H_5O^-$	10.0		0.3
$C_6H_4(NH_2)O^-$	10.0		40
$SSal^{3-}$	12.0		0.6[d]
Sal^{2-}	13.1		0.7

[a] Outer-sphere association constants at $I = 0.1$ are estimated for various charge types to be as follows: $K_{os} \cong 0.3$, 2, 5, and 100 for the product of charges $(z_A z_B) = 0$, −2, −3, and −6, respectively. In the absence of further information, these values, as rough estimates, were used at higher ionic strengths as well. As a consequence the values of k_{1p} are significant to one digit only. [b] L form shown; pK_a is for the ionization of the corresponding HL form. [c] A directly measured value. [d] Computed with an outer-sphere constant for a 2–1 charge type. The additional 1− charge imparted by the $-SO_3^-$ group does not appear to enhance the electrostatic attraction. See ref 9b.

Let us now reanalyze the situation without making any *a priori* assumptions. First, if one were to accept pathway 1 for the ambiguous systems, he would have to assume that the iron reactions follow this path and then, at some limit in basicity of the ligand, suddenly switch to pathway 5. This is shown by the fact that the computed k_1 values increase to beyond 10^{10} M^{-1} sec^{-1}, which is the diffusion limit. At that point (systems with $pK > \sim 8$) it would be necessary to attribute rate processes to the k_5 path, for which smaller values are computed.

Second, the apparent correlation of k_1 with ligand basicity provides no support for the k_1 assignment, because (for a monoprotonated ligand) the observed rate can be written

$$\frac{d[FeL]}{dt} = (k_1(K_a/K_{OH}) + k_5)[FeOH][HL] = k_{obsd}[FeOH][HL]$$

If one attributes the rate to the k_1 term, then it is obvious that $k_1 = k_{obsd}K_{OH}/K_a$. As a consequence, if k_{obsd} is approximately constant, then *computed* k_1 values will necessarily increase as the pK_a of the attacking ligand increases.

Third, Table V lists the ligand penetration rate constants for our systems, as well as those from other studies in which the data are calculated for both pathway 1 and pathway 5. It is seen that Cl^-, Br^-, and SCN^- systems can be unambiguously associated with k_1 values. These ligands do not ordinarily protonate and therefore have to follow pathway 1. Their rate constants are in the order of 10^1 sec^{-1}, whereas the k_{1p} values computed for the ambiguous ligands are very much larger. We were able, for phenol and *o*-aminophenol, unambiguously to assign the reaction to pathway 5, involving $FeOH^{2+}$ + HL. Values of k_{1p} cluster for the most part about 3×10^4 sec^{-1}, but there is considerable variation. They do not however correlate with basicity of the HL form. Finally, the value of k_{H_2O}, the water-exchange lifetime for $FeOH^{2+}$, has been reported[19] to be approximately 10^{-4} sec. This is

---

(17) G. G. Davis and W. M. Smith, *Can. J. Chem.*, **40**, 1836 (1962).

(18) H. Wendt and H. Strehlow, *Z. Elektrochem.*, **66**, 228 (1962).

(19) R. E. Connick and E. E. Genser, as quoted by Seewald and Sutin.[12]

consistent with the data in Table V. Although the relative constancy of k_{1p} does not establish the pathway as being FeOH + HL for all these systems, this fact, plus the other observations, argues for the assignment of the rate constants to k_5 as indicated in Table V. If k_{1p} is on the order of 10^1 $\sec^{-1}$ for the k_1 pathway, then the contributions from this pathway to the measured rate would be quite small for ligands which are mostly protonated in acid solutions.

Acknowledgment. This work was supported by the National Science Foundation in the form of a Departmental Undergraduate Research grant to S. G. and by the National Institutes of Health in the form of a research grant to J. S. (GM-13116).

Registry No. Fe^{3+}, 20074-52-6; C_6H_5OH, 108-95-2; o-$H_2NC_6H_4OH$, 95-55-6.

Contribution from the Department of Chemistry,
Texas A&M University, College Station, Texas 77843

Iron(III) Chelate Complexes of Hydrogen Sulfide and Mercaptans in Aqueous Solution

C. V. PHILIP[1] and DAVID W. BROOKS*

Received June 29, 1973

Iron(III) *N*-hydroxyethylethylenediaminetriacetate (Fe^{III}HEDTA) and other iron(III) chelates react with hydrogen sulfide and mercaptans in aqueous solution. Unstable pink complexes form. Fe^{III}HEDTA forms a complex with 2 mol of iron chelate per mole of H_2S ($K = 4.4 \times 10^6$; λ_{max} 490 nm; ϵ_{max} 8900). With other mercaptans (mercaptoethanol, ethyl mercaptan, L-cysteine), 1:1 complexes are formed ($K = 10$; λ_{max} 530 nm; ϵ_{max} 3200). The stoichiometry of the complex is assigned on the basis of an iterative procedure applied to spectrophotometric data determined for maximum extent of complex formation. Esr spectra of these complexes show a sharp peak superimposed upon a broad peak at $g = 4.3$.

Introduction

The structure and the hydrolytic properties of the iron(III) chelate of *N*-hydroxyethylethylenediaminetriacetic (HEDTA) have been extensively studied.[2-6] In view of the preceding work on the aqueous iron(III) chelate systems, it seemed reasonable to assume that these complexes contained a *hard core primary coordination polyhedron* at iron with at least one available uncoordinated or weakly coordinated position which could readily accommodate a good nucleophilic ligand. We were interested in the reactions of these iron chelates with hydrogen sulfide and mercaptans in aqueous solution.

Experimental Section

Chemicals. Chemicals were obtained from the following sources: potassium chloride, ferric sulfate, and ferrous sulfate from Fisher Scientific Co.; HEDTA from Eastman Co.; $Na_2EDTA \cdot 2H_2O$ from J. T. Baker Chemical Co.; hydrogen sulfide from Matheson Co.; 2-mercaptoethanol and ethyl mercaptan from Pfaltz and Bauer, Inc.; L-cysteine hydrochloride, mercaptoacetic acid, and methyl mercaptan (gaseous) from Aldrich Chemical Co. All chemicals were used without further purification.

Solutions. All solutions were made in deionized distilled water which had been deoxygenated by bubbling with nitrogen. Once prepared, solutions were again bubbled with nitrogen and stored under a nitrogen atmosphere. Ferric HEDTA solution was made from standardized ferric sulfate and standardized HEDTA solutions. The pH of chelate solutions was adjusted by adding 2.0 *M* NaOH. In order to maintain constant ionic strength during each study, 0.4 mol of KCl was added per liter of the solution. Also, a 2% excess of HEDTA was maintained in the ferric HEDTA solutions. Similarly, ferric EDTA solutions were made by mixing standardized solutions of ferric sulfate and EDTA, etc.

Saturated solutions of ethyl mercaptan were made in cold water. Gaseous methyl mercaptan was dissolved in ice-cold water. L-Cysteine hydrochloride (99%) was dissolved in water and sufficient NaOH was added to raise the pH to 7. Dilutions to required strength were made from this stock solution.

Hydrogen sulfide wad dissolved in cold nitrogen-saturated water and diluted to required concentration. All mercaptan and hydrogen sulfide solutions were standardized by titration with standardized silver nitrate solution using silver electrode potentiometric end point detection.

Flow System. Since the complexes formed between iron(III) chelates and sulfur ligands are inherently unstable, all the spectrophotometric studies were carried out using a specially devised flow system consisting of two cylindrical reservoirs of identical diameter, each with a capacity of 2 l. and a height of about 20 in. A constant pressure of 14 psi could be maintained by connecting the upper reservoir inlets to a nitrogen supply. Two liters each of standardized solutions of iron(III) chelate and mercaptan were stored in separate wash bottles. The solutions were transferred into the reservoirs *via* lower reservoir inlets by nitrogen pressure. The separate solutions of iron(III) chelate and mercaptan or hydrogen sulfide were mixed using a four-jet mixing chamber (Varian Associates) and allowed to flow through a quartz spectrophotometer cell of 5.0-mm path length. The visible spectra of the resulting solutions were scanned at various flow rates using a Cary 14 spectrophotometer. The dead time (time for flow between mixer and cell) was 0.1 sec at 5 ml/sec flow rates. Spectra were obtained at 25 ± 1° in the presence of 0.2 *M* KCl. Other salts (KNO_3, K_2SO_4) proved equally effective at maintaining ionic strength.

The effluent from the flow cell was passed through a small cell containing a glass electrode and KCl bridge to a standard calomel electrode allowing pH determination.

For every pair of iron(III) chelate and mercaptan (or H_2S) concentrations, the stopped-flow spectrophotometric recordings were repeated ensuring reproducibility. When absorbance was measured at constant wavelength (490 or 530 nm), absorption maximum was reached shortly after the flow was stopped and decay of the absorbance with time was easily measured.

Esr Studies. Esr experiments were performed using a Varian E-6S spectrometer. An esr flow system was used for mixing the solution.[7] One end of an open ended quartz tube was attached to

---

* Address correspondence to this author at Department of Chemistry, University of Nebraska, Lincoln, Nebr. 68508

(1) Taken in part from the Ph.D. dissertation of C. V. Philip, Texas A&M University, 1972. Fellow of the Robert A. Welch Foundation, 1969-1972.

(2) R. L. Gustafson and A. E. Martell, *J. Phys. Chem.*, **67**, 576 (1963).

(3) H. Schugar, C. Walling, R. B. Jones, and H. B. Gray, *J. Amer. Chem. Soc.*, **89**, 3712 (1967).

(4) H. J. Schugar, A. T. Hubbard, F. C. Anson, and H. B. Gray, *J. Amer. Chem. Soc.*, **91**, 71 (1969).

(5) H. J. Schugar, G. R. Rossman, and H. B. Gray, *J. Amer. Chem. Soc.*, **91**, 4564 (1969).

(6) H. J. Schugar, G. R. Rossman, C. G. Barraclough, and H. B. Gray, *J. Amer. Chem. Soc.*, **94**, 2683 (1972).

(7) E. L. Lewis and F. Sicilio, *J. Phys. Chem.*, **73**, 2590 (1969).